J. Membrane Biol. 112, 255–265 (1989)

The Journal of
Membrane Biology

Effects of Calcium and Bay K-8644 on Calcium Currents in Adrenal Medullary Chromaffin Cells

Valentin Ceña*, Andres Stutzin**, and Eduardo Rojas
Laboratory of Cell Biology and Genetics, National Institute of Diabetes and Digestive and Kidney Diseases, National Institutes of Health, Bethesda, Maryland 20892

Summary. The kinetic and steady-state characteristics of calcium currents in cultured bovine adrenal chromaffin cells were analyzed by the patch-clamp technique. Whole cell inward Ca^{2+} currents, recorded in the presence of either 5.2 or 2.6 mM Ca^{2+} exhibited a single, noninactivating component. To analyze the effects of Ca^{2+} and Bay K-8644 on the kinetics of the Ca^{2+} currents, we used a modified version of the Hodgkin-Huxley empirical model. At physiological $[Ca^{2+}]$ (2.5 mM) the midpoint of the steady-state Ca^{2+}-channel activation curve lay at −6.9 mV. Increasing the $[Ca^{2+}]$ to 5.2 mM shifted the midpoint by −4.3 mV along the voltage axis. At the midpoint, changes in potential of 7.8 mV (for 5.2 mM Ca^{2+}) and 9.2 mV (for 2.5 mM Ca^{2+}) induced an *e*-fold change in the activation of the current. Increasing $[Ca^{2+}]_o$ from 2.5 to 5.2 mM induced a marked increase in the rate constant for turning on the Ca^{2+} permeability. Conductances were estimated from the slope of the linear part of the current-voltage relationships as 8.7 and 4.2 nS in the presence of 5.2 and 2.5 mM Ca^{2+}, respectively. Incubation of the cells in the presence of Bay K-8644 at increasing concentrations from 0.001 to 0.1 μM increased the slope conductance from 4.2 to 9.6 nS. Further increases in the concentration of Bay K-8644 from 1 to 100 μM induced a marked reduction in the conductance to 1.1 nS. In the presence of Bay K-8644 (0.1 μM) the midpoint of the activation curve was shifted by 6.1 mV towards more negative potentials, i.e., from −6.9 to −13 mV. At the midpoint potential of −13 mV, a change in potential of 6.9 mV caused an *e*-fold change in Ca^{2+} permeability. The kinetic analysis showed that Bay K-8644 significantly reduced the size of the rate constant for turning off the Ca^{2+} permeability.

Key Words Ca^{2+} channel · Bay K-8644 · chromaffin cell · Ca^{2+} current · catecholamine secretion · medullary cell · Ca^{2+}-channel gating

Introduction

Acetylcholine and high K^+ induce secretion of catecholamines (CA) from adrenal medullary chromaffin cells in culture (Schneider et al., 1981; Baker & Knight, 1984), and the secretory response is absolutely dependent on extracellular calcium ($[Ca^{2+}]_o$) (Holz, Senter & Frve, 1982; Heldman et al., 1989). The crucial problem involved in analysis of calcium-dependent CA secretion now includes understanding the mechanisms by which specific receptors can induce elevation of cytosolic calcium concentration ($[Ca^{2+}]_i$). It has become apparent that the calcium responsible for the elevation in intracellular calcium during cholinergic activation of the chromaffin cells originates both from intra- and extracellular sources (Kidokoro & Ritchie, 1980; Kao & Schneider, 1985), and the relative magnitudes of these contributions depend on the dose and the type of cholinergic agonist used (Forsberg, Rojas & Pollard, 1985; Rosario et al., 1989). A rapid elevation of $[Ca^{2+}]_i$ occurs immediately after occupancy of either cholinergic nicotinic or muscarinic receptors (Rosario et al., 1989). While nicotinic receptors modulate the entry of Ca^{2+} from the external medium, muscarinic receptors elicit the release of Ca^{2+} from intracellular pools as a consequence of inositol trisphosphate production through a common receptor-operated transduction process. The process appears to involve phospholipase C-catalyzed hydrolysis of membrane phosphoinositides (Forsberg et al., 1985; Pollard et al., 1986). High K^+ causes secretion by depolarizing the membrane, which in turn activates voltage-gated Ca^{2+} channels. The value of high K^+-induced secretion is that it allows analysis of voltage-gated Ca^{2+} pathways relevant to secretory processes.

Earlier studies using the patch-clamp technique demonstrated the presence of voltage-dependent, noninactivating Ca^{2+} channels in cultured bovine adrenal chromaffin cells (Fenwick, Marty & Neher, 1982*a*,*b*). Further support for the idea that this Ca^{2+} channel was involved in CA secretion evoked by a sudden elevation of extracellular K^+ was provided

* *Present address:* Department of Neurochemistry, Faculty of Medicine, University of Alicante, Alicante, Spain.
** *Present address:* Department of Experimental Medicine, Faculty of Medicine, University of Chile, Santiago, Chile.

by the observation that Ca^{2+}-channel agonist (Bay K-8644) and antagonists (nifedipine and nitrendipine) respectively enhance or reduce CA release in response to high K^+ or cholinergic agonists (Ceña et al., 1983; Garcia et al., 1984; Heldman et al., 1989).

The purpose of our present work was to determine the kinetic and steady-state characteristics of the noninactivating Ca^{2+} channel known to be present in bovine adrenal chromaffin cells. Analysis of the time course of the Ca^{2+} permeability increase in response to membrane depolarization confirmed the existence of a single delayed component. Since the Ca^{2+} current was sensitive to Bay K-8644, we proposed that chromaffin cells are equipped with Ca^{2+} channels of the L type (Tsien et al., 1987; Kaczmarek, 1988).

Materials and Methods

Preparation of the Chromaffin Cells

Chromaffin cells were prepared from bovine adrenal medulla by a modified collagenase digestion method similar to that described previously in detail (Greenberg & Zinder, 1982). After further separation of the chromaffin cells using a percoll gradient (Kilpatrick et al., 1980), they were placed in Eagle's essential medium at a concentration of 2 million cells per dish (35 mm, Corning) and allowed to recover from the isolation procedure for a 3-day period in a CO_2 incubator at 37°C. After this incubation the cells were ready for patch-clamp measurements.

Electrical Measurements

Pipettes were prepared from micro-hematocrit capillary tubes (i.d. 1.1–1.2 mm, wall thickness 0.2 mm) using a BB-CH microelectrode puller (Mecanex S.A., Geneva, Switzerland). For those experiments in which membrane capacity was measured and used to normalize the current, the tip of the pipettes was fire polished and coated almost to the tip with Sylgard (184 Elastomer kit, Dow Corning, Midland, MI). These pipettes had an open-tip resistance in the range from 1.5 to 3.5 MΩ, and when the cell-attached seal was formed the resistance rose to 20–50 GΩ. Current transients were recorded under voltage-clamp conditions using a List EPC-7 amplifier (List-Electronics, Darmstadt-Eberstadt, FRG).

Experimental Protocol

Whole-cell currents were recorded at room temperature (18–23°C). Once a satisfactory seal was established (>20 GΩ), the capacity transient was compensated for, and then the membrane patch was broken by applying gentle suction to the pipette. Immediately after the whole cell recording configuration was established, the membrane potential was measured under current clamp conditions. As a rule, the values measured fell in the range from −45 to −65 mV. Since the solution used to dialyze the cell interior (in mM: 75 Cs Glutamate, 75 CsCl, 2 Mg-ATP, 10 Na-HEPES, 1 $CaCl_2$, 10 CsEGTA, pH = 7.2) blocked K^+ channels, the membrane potential decreased with time (<3 min) to about −40 mV. Under voltage-clamp conditions, the holding potential was adjusted to −80 mV. At this time we estimated the value of the cell capacitance and the size of the resistance in series with the membrane R_s (5–6 MΩ) as described elsewhere (Sakmann & Neher, 1983). Membrane capacity, measured as the extra capacity acquired with the whole cell configuration, ranged from 6 to 8 pF. Since for the present series of experiments we used Na-free extracellular solutions (in mM: 140 CholineCl, 1 $MgCl_2$, 2.5 or 5.2 $CaCl_2$, 5 KCl, 10 CsHEPES, pH = 7.4), the fast and large inward Na^+ current was absent from our records (Fenwick et al., 1982*a*,*b*). In perfect agreement with previous work (Fenwick et al., 1982*a*,*b*), the absolute size of the inward current was always smaller than 0.5 nA. Complete correction for the effects of this resistance in series would be achieved on-line by positive feedback of a voltage V_s equal to the product of the time varying current $i(t)$ and R_s. Thus, for an estimated value of R_s smaller than 6 MΩ, the maximum V_s that would adequately compensate for the effects of R_s would be 3 mV. A comparison of the currents in the presence (experiments with 2.5 mM Ca^{2+}) or absence (experiments with 5.2 mM Ca^{2+}) revealed that both the kinetic and steady-state characteristics of the inward currents were unaffected by the R_s compensation (*see* Results).

A digital computer (System 90, Computer Instrumentation, South Hampton, U.K.) was used on-line to generate voltage pulses and to record the current signal. Current transients were low-pass filtered (corner frequency set at 10 kHz) to a 12-bit analog-to-digital converter. Voltage pulse protocols were under computer control, and the current signal was digitized at 70 μsec sampling intervals. Each record was stored on digital magnetic tape using a method that enabled us to store records consisting of 3072 samples in 500 msec. The single pulse procedure was used to acquire a series of current records at different membrane potentials. During each cycle (0.25–0.5 Hz) either two rectangular pulses of identical size, but opposite polarity (±10, ±20, ±30, ±40 and ±50 mV) or two pulses of different size and opposite polarity (60/−50, 70/−50, . . . , 140/−50 mV) were applied. Each record of the membrane currents consisted of three consecutive segments: the first segment (4.48 msec) at the holding potential was acquired to form a baseline; the second segment (typical duration 103 msec) at the membrane potential during the pulses was acquired to obtain the nonlinear components of the membrane currents, and the third segment (typical duration 107 msec) at the holding potential was acquired to obtain the tail currents.

The same computer was used after the experiments for off-line analysis of the records. Before starting the analysis, each record was treated as follows: (i) The holding current before the test and control pulses (base line) was evaluated. (ii) Test pulses were always in the depolarizing direction. The control pulse could be either in the depolarizing or in the hyperpolarizing direction. However, for all the experiments presented here, a record of the membrane currents in response to a fixed pulse (20 mV) was used as a control record. The test pulse and the control pulse current transients (after proper scaling of the control pulse transient) were summed. (iii) Several pairs (2–5) were averaged. (iv) The 3072 points in each averaged record were condensed into 1024 values by averaging again each subsequent three points.

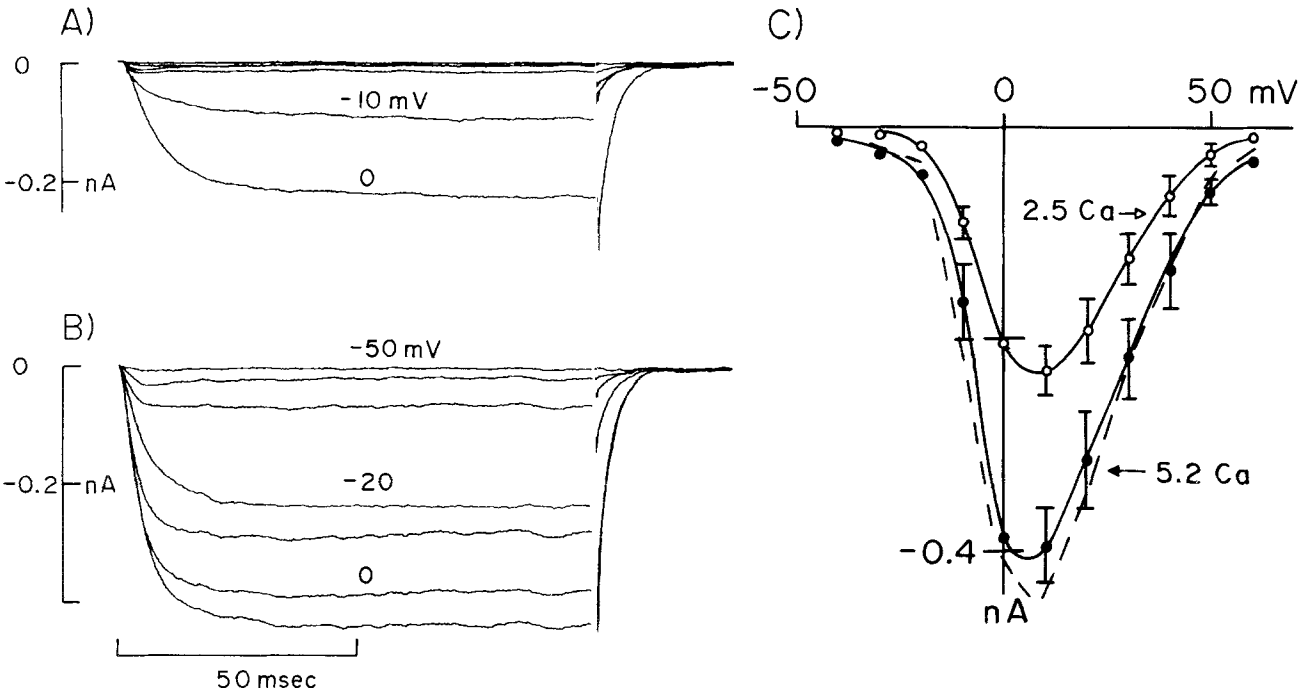

Fig. 1. Time course of the inward currents at different membrane potentials. Superimposed Ca^{2+} current records corrected for capacity transients and leakage currents as described in Materials and Methods. (*A*) Chromaffin cell internally dialyzed with K^+-free solutions (Cs^+ in place of K^+). The external Na^+-free solution ($Choline^+$ in place of Na^+) contained 2.5 mM Ca^{2+}. Temperature about 20°C. (*B*) Inward currents from another chromaffin cell bathed in Na^+-free medium containing 5.2 mM Ca^{2+}. Temperature ca. 20°C. (*C*) Current-voltage relationships in 2.5 (○) and 5.2 (●) mM $[Ca^{2+}]_o$. Symbols represent the mean values of nine experiments on different cells at 2.5 mM $[Ca^{2+}]_o$ and four experiments on different cells at 5.2 mM $[Ca^{2+}]_o$. Vertical bars represent 2 SEM. Conductances (estimated from the linear parts at 10 through 40 mV) were 4.2 (○) and 8.7 (●) nS, respectively. Dashed curve represents the predicted size of the current at 5.2 mM $[Ca^{2+}]_o$ and was generated using Eq. (1b) (*see* text) and the data points obtained at 2.5 mM (○)

Results

Voltage-Dependent Calcium Currents Exhibit a Single Component

Figure 1 depicts two sets of superimposed membrane current records from a chromaffin cell internally dialyzed with K^+-free Cs^+ solution and bathed in a modified Krebs buffer (in mM: 140 CholineCl, 5 KCl, 1 $MgCl_2$, 10 NaHEPES, pH 7.4) in the presence of either 2.5 (*A*) or 5.2 mM $CaCl_2$ (*B*). At each membrane potential the inward current gradually increased, reaching a maximum level which remained constant until the end of the pulse (107 msec). These characteristics of the conductance increase suggest the presence of a single voltage-dependent pathway for Ca^{2+} entry in the chromaffin cell membrane. Figure 1*C* shows the corresponding current-voltage relationships (*I-V* curves). Increasing $[Ca^{2+}]_o$ from 2.5 to 5.2 mM had no effect on the kinetics of the currents. However, the size of the current increased (Fig. 1*C*), as predicted on the basis of the assumption of independence (Hodgkin & Huxley, 1952*a*) and constant field (Hodgkin & Katz, 1949). We may write

$$P_{Ca} = i_{Ca}\{RT/4F^2\}\{1/[Ca]V\}\{(e^{2VF/RT} - 1)/(e^{2(V-V_{eq})F/RT} - 1)\} \quad (1a)$$

where P_{Ca} represents the permeability to Ca^{2+}, V_{eq} represents the equilibrium potential and R, T, F have their usual meanings. Assuming that at each membrane potential P_{Ca} remains constant, the ratio of the current i_{Ca} recorded at 2.5 mM over the current i^*_{Ca} recorded at 5.2 mM should be

$$i_{Ca}/i^*_{Ca} = [Ca^{2+}]/[Ca^{2+}]^*\{(e^{2(V-V_{eq})F/RT} - 1)/(e^{2(V-V^*_{eq})F/RT} - 1)\} \quad (1b)$$

where i_{Ca}, $[Ca^{2+}]$ represent the steady-state current and the external concentration of Ca^{2+} for the control and, i^*_{Ca}, $[Ca^{2+}]^*$ are the corresponding values for the test run. Assuming that

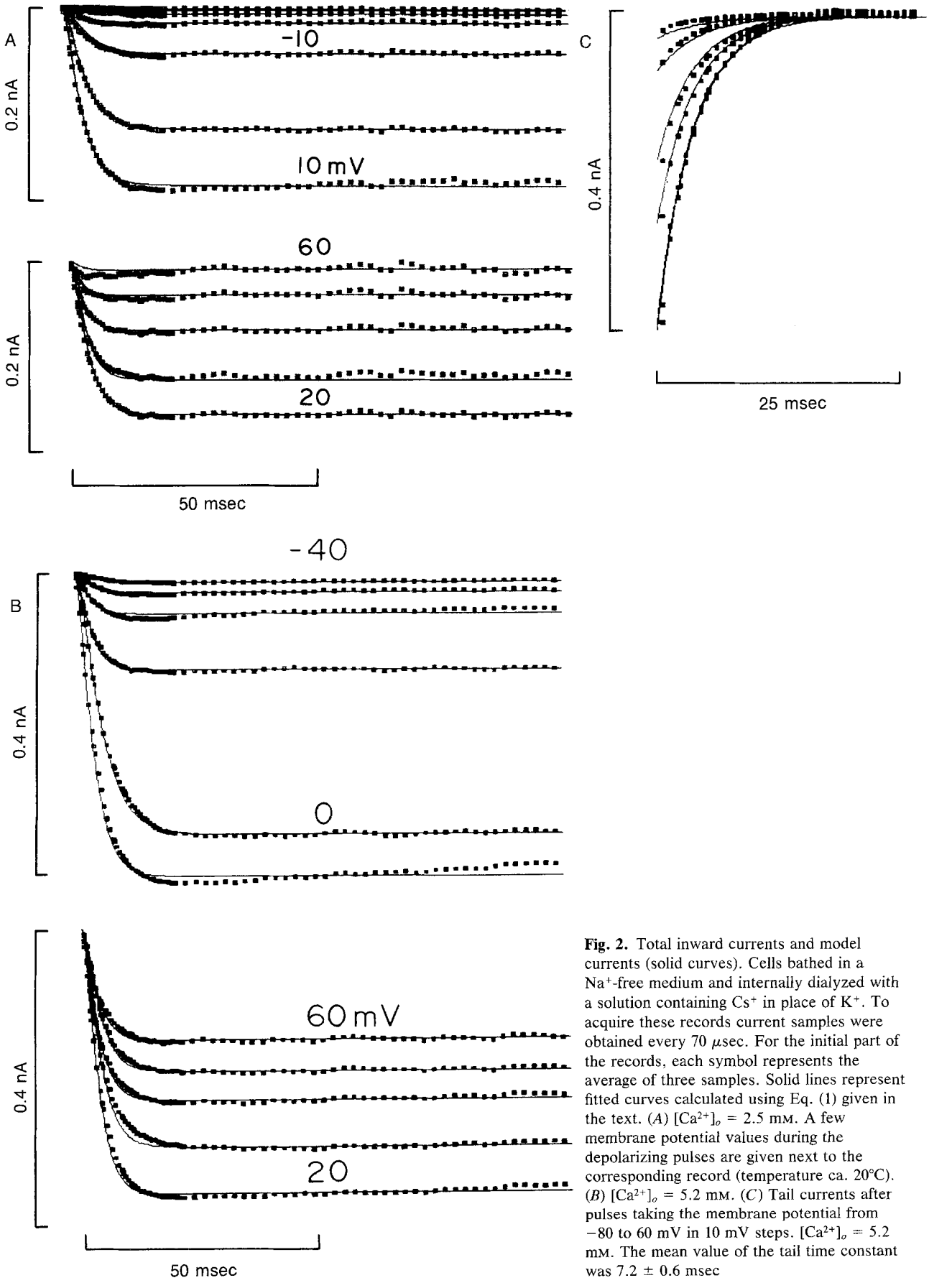

Fig. 2. Total inward currents and model currents (solid curves). Cells bathed in a Na^+-free medium and internally dialyzed with a solution containing Cs^+ in place of K^+. To acquire these records current samples were obtained every 70 μsec. For the initial part of the records, each symbol represents the average of three samples. Solid lines represent fitted curves calculated using Eq. (1) given in the text. (*A*) $[Ca^{2+}]_o$ = 2.5 mM. A few membrane potential values during the depolarizing pulses are given next to the corresponding record (temperature ca. 20°C). (*B*) $[Ca^{2+}]_o$ = 5.2 mM. (*C*) Tail currents after pulses taking the membrane potential from −80 to 60 mV in 10 mV steps. $[Ca^{2+}]_o$ = 5.2 mM. The mean value of the tail time constant was 7.2 ± 0.6 msec

$$V_{eq} = RT/2F \ln \{[Ca^{2+}]_o/[Ca^{2+}]_i\}, \quad (2)$$

for a $[Ca^{2+}]_i$ of 50×10^{-9} M, V_{eq} is calculated as 135 and 144 mV at $[Ca^{2+}]_o$ of 2.5 and 5.2 mM, respectively. Dashed curve was calculated using Eq. (1b).

Conductances were estimated from the slope of the linear part of the *I-V* curves as 4.2 and 8.7 nS in the presence of 2.5 and 5.2 mM $[Ca^{2+}]_o$, respectively.

Analysis of the Inward Ca^{2+} Current Kinetics

The steady-state and kinetic characteristics of the Ca^{2+} currents were determined by the approach previously used by us (Stutzin et al., 1989) and others (Quinta-Ferreira, Rojas & Arispe, 1982), i.e., the empirical Hodgkin-Huxley (1952*b*) formalism. Figure 2 shows that it is possible to accurately fit all the inward current records by assuming the presence of a single component of the current. We may write

$$i_{Ca}(V) = i_{Ca,max}(V)\{1 - \exp[-t/\tau(V)]\}^2 \quad (3)$$

where $\tau(V)$ represents the time constant for activation and $i_{Ca,max}(V)$ the steady-state level of the current at each membrane potential V. For this analysis, the records were corrected for leakage and linear capacity currents (*see* Materials and Methods). Steady-state and activation time constant values were obtained from the least squares regression fit illustrated in Fig. 2. The goodness of the fit was evaluated using a computer program designed to minimize the sum of the squared differences between the measured and the predicted values. Figure 2 shows two sets of fitted curves calculated with Eq. (1) (solid lines) together with the corresponding current record made in the presence of 2.5 (*A*) or 5.2 mM Ca^{2+} (*B*). Also shown in Fig. 2*C* are the tail currents recorded after the pulses in the presence of 5.2 mM Ca^{2+}.

We can define the time constant of activation in terms of the rate constants for a single transition between two states, i.e., $\alpha(V)$ and $\beta(V)$ as

$$\tau(V) = 1/\{\alpha(V) + \beta(V)\} \quad (4)$$

and the fraction of the Ca^{2+} channels in open configuration in the steady state (or open probability) $m_\infty(V)$ as

$$m_\infty(V) = \alpha(V)/\{\alpha(V) + \beta(V)\}. \quad (5)$$

The midpoint for the steady-state $m_\infty(V)$ function calculated from the data obtained in the presence of 2.5 mM Ca^{2+} (Fig. 3*A*, ○) lay at −6.9 mV and 9.8 mV induced an *e*-fold change in $m_\infty(V)$ at this potential. At 5.2 mM Ca^{2+} (Fig. 3*A*, ●) the corresponding values were −11.2 and 8.5 mV.

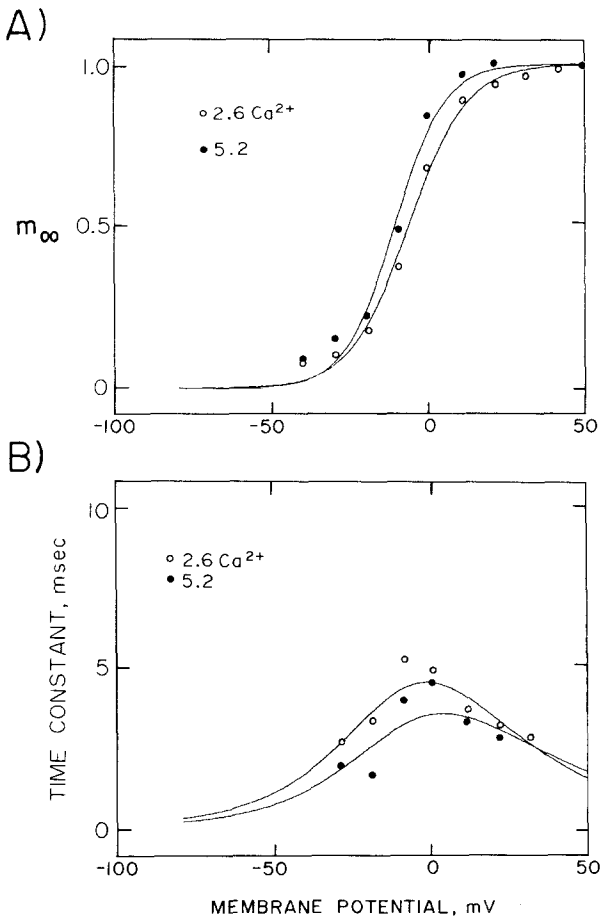

Fig. 3. Steady-state open Ca^{2+}-channel *m*-gate and time constant curves. (*A*) m_∞ values were obtained from the *I-V* curves. Continuous curves were calculated with the following equation:

$$m_\infty = 1/\{1 + \exp[a(V - V_o)/kT]$$

where kT was taken as 25.3 meV. Parameters from the best fit:

$[Ca^{2+}]_o = 2.5$, $a = -2.7$; $V_o = -6.9$ mV.

$[Ca^{2+}]_o = 5.2$, $a = -3.2$; $V_o = -11.2$ mV.

(*B*) Fitted time constant curves were calculated using the equations given in the text with the following parameters for the best fit: At 2.5 mM Ca^{2+}, $A = 96.1$ sec^{-1}, $a = -0.74$, $V_o = -14.8$ mV; $B = 35$ sec^{-1}, $b = -1.22$, $V_o = -15.1$ mV. At 5.2 mM Ca^{2-}, $A = 144.4$ sec^{-1}, $a = -0.57$, $V_o = -9.9$ mV; $B = 47.32$, $b = -1.25$, $V_o = -14.9$ mV

Equations (4) and (5) were resolved for $\alpha(V)$ and $\beta(V)$. Shown in Fig. 4 are the values of the rate constants at 2.5 (*A*) and 5.2 mM Ca^{2+} (*B*). The curves represent the best fit to the points and were calculated using exponential rate functions of the form

$$\alpha(V) = A \exp[a(V - V_o)] \quad (6a)$$

$$\beta(V) = B \exp[b(V - V_o)] \quad (6b)$$

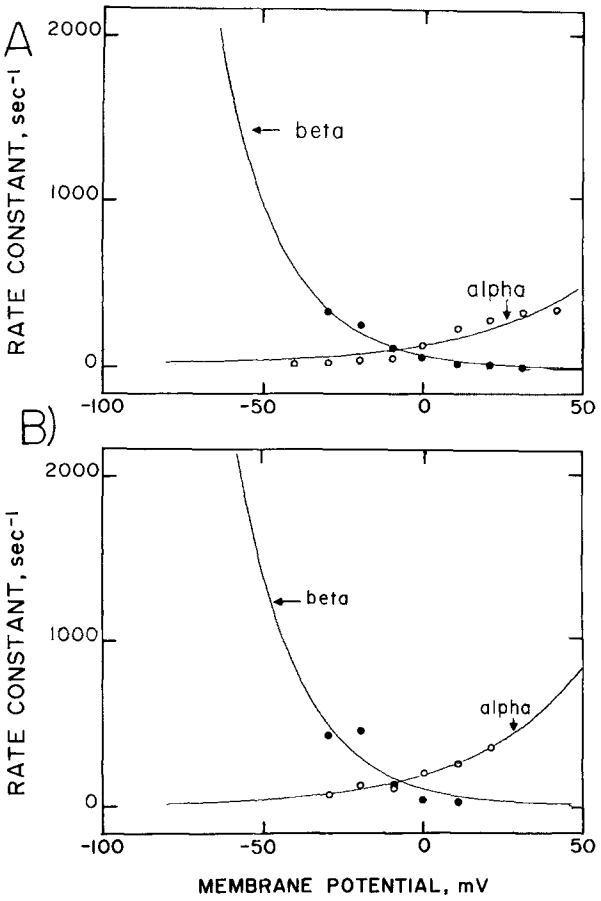

Fig. 4. Effect of increasing $[Ca^{2+}]$ from 2.5 to 5.2 mM on rate constants. (*A*) Rate constants in the presence of 2.5 mM $[Ca^{2+}]_o$. Parameters for the best fit as follows: $A = 96.1$ sec^{-1}, $a = -0.66$ electronic charges and $V_o = -14.8$ mV. $B = 46.4$ sec^{-1}, $b = -1.25$ electronic charges and $V_o = -14$ mV. (*B*) Rate constants in the presence of 5.2 mM $[Ca^{2+}]$. Parameters: $A = 144.4$ sec^{-1}, $a = -0.75$ electronic charges and $V_o = -10$ mV. $B = 47.4$ sec^{-1}, $b = -1.3$ electronic charges and $V_o = -15$ mV

where a (or b) and V_o have their usual meaning. The values of the time constants are shown in Fig. 3*B* together with the continuous curve calculated with Eqs. (4), (5) and (6*a*,*b*). The parameters that gave the best fit are given in the legend to Figs. 3 and 4.

Bay K-8644 Enhances Ca^{2+} Inward Currents

The Ca^{2+}-channel agonist Bay K-8644 potentiates Ca release evoked by high $[K^+]_o$ in adrenal medullary chromaffin cells (Garcia et al., 1984). Consistent with these results we found that Bay K-8644 (0.1 μM) potentiates inward Ca^{2+} currents in a dose-dependent manner (Figs. 5–7). Maximum enhancement was achieved at 0.1 μM (Figs. 6 and 7). Internal application of Bay K-8644 alone (0.1 μM) also enhanced inward Ca^{2+} currents (Fig. 6*B*, ●). Doses

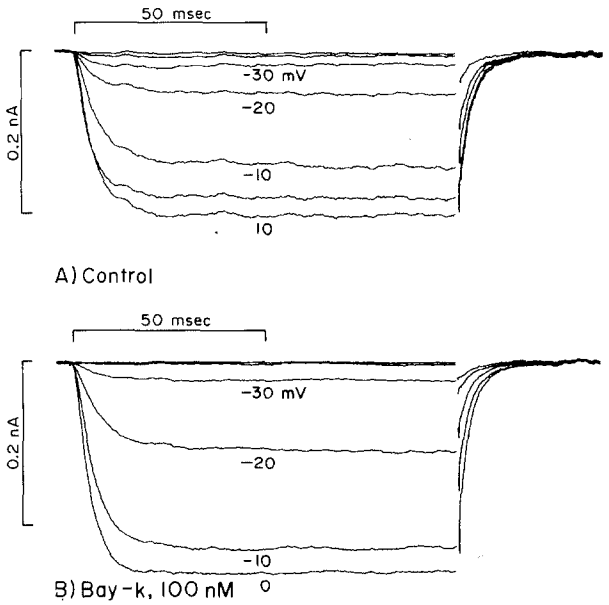

Fig. 5. Effect of BAY K-8644 on inward currents. Inward current kinetics in the above (*A*) or in the presence (*B*) of BAY K-8644 (0.1 μM). Membrane potential during some of the depolarizing pulses are given in mV next to the corresponding current record

of the dihydropyridine higher than 0.1 μM always inhibited the inward currents (Figs. 6 and 7). While half maximal enhancement was achieved at a concentration of Bay K-8644 of about 0.03 μM, half maximal inhibition was observed at a concentration of the dihydropyridine of ca. 1 μM (Fig. 7).

Bay K-8644 Reduces the Rate Constant for Turning Off Ca^{2+} Current

The analysis of the currents shown in Figs. 2*A–C* suggested that it is possible to modify the Hodgkin-Huxley empirical model to describe the kinetics of the Ca^{2+} current in chromaffin cells. The experiments summarized in Figs. 5–7 clearly show that in the presence of Bay K-8644 at concentration smaller than 0.1 μM the size of the steady-state Ca^{2+} currents in substantially greater than in the absence of the Ca^{2+}-channel agonist. There are three possible explanations for this result: (i) An increase in the size of the unitary Ca^{2+}-channel current; (ii) an increase in the size of the rate constant for turning on the Ca^{2+} channel or/and (iii) a decrease in the rate for turning off the Ca^{2+} channel. To distinguish between these alternatives we determined the steady-state and kinetic parameters in the presence of Bay K-8644 (Fig. 8).

From this analysis we obtained the $m_\infty(V)$ and $\tau(V)$ curves as shown in Fig. 9*A*,*B*. To facilitate the

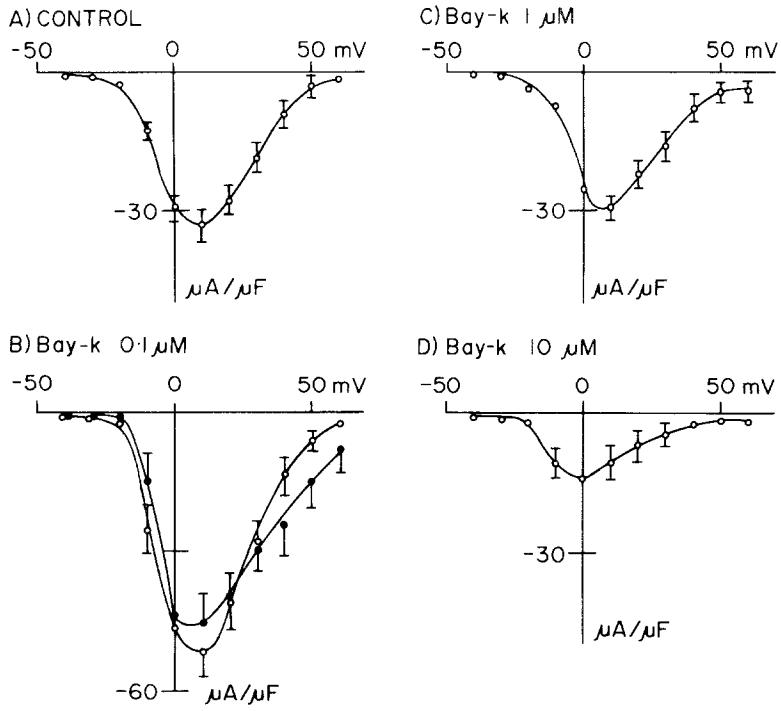

Fig. 6. Current-voltage relationships in the presence of increasing concentrations of BAY K-8644. Vertical axis represents the ratio "whole cell current in μA/whole cell membrane capacity in μF" measured as described in the Method section. Symbols represent the mean values from 12 (A), 4 (B), 4 (C) and 5 (D) different cells. Comparison of the effects of Bay K-8644 at 0.1 μM internally (●) and externally (○) applied. Vertical bars represent 2 SEM

comparison with the control curves we have plotted them in the same graph. It may be seen that the effect of Bay K-8644 can be expressed as an increase in the effective valence "a" from −2.7 to −3.6 electronic charges and a shift in the transition potential from −6.9 to −12.9 mV. Thus, the voltage sensitivity of the channel is increased from 9.8 to 7 mV for an e-fold change in m_∞ at the midpoint. Figure 9*B* illustrates the moderate changes in the time constant $\tau(V)$ of activation of the Ca^{2+} current by the Ca^{2+}-channel agonist. It may be seen that both in the absence or presence of Bay K-8644 the time constants are rather similar for positive potentials. However, for negative potentials the time constants in the presence of Bay K-8644 are substantially greater (Fig. 9*B*, ●). To further distinguish the effects of the Ca^{2+}-channel agonist we have resolved Eqs. (2) and (3) for $\alpha(V)$ and $\beta(V)$. Figure 9*C* clearly shows that the rate constant for turning off the Ca^{2+} current is reduced at negative potentials in the presence of Bay K-8644. This means that the open time of the Ca^{2+} channel is increased.

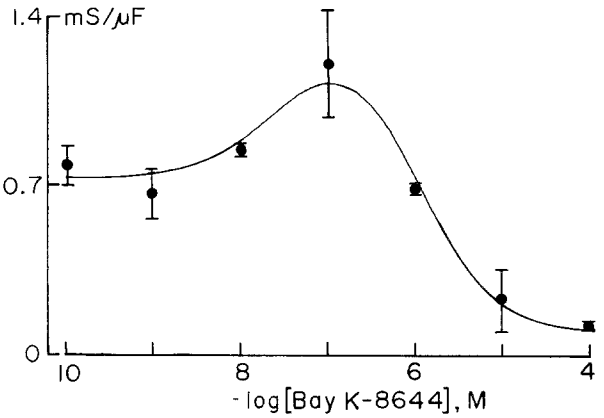

Fig. 7. Dose-response curve for BAY K-8644 in terms of the steady-state chord conductance measured at 10 mV. Each symbol represents the mean value (±SEM) of the chord conductance for the inward calcium current (from 4 to 12 different cells). Ordinate represents the ratio

$$i_{Ca,max}(V = 10 \text{ mV})/-42 \text{ mV}$$

in mS/μF. The "apparent" reversal potential was estimated as the intercept of the extrapolated linear segment of the *I-V* curve on the *V* axis, i.e., 52 mV. The curve was calculated using the occupancy model described in the Discussion. The values which gave the best fit were as follows: $g_{Ca,max} = 0.64$ mS/μF; $K_{D,1} = 0.027$ μM; $K_{D,2} = 1.04$ μM; $g^*_{Ca} = 0.1$ mS/μF

Discussion

One Type of Voltage-Dependent Ca^{2+} Channel is Present in the Chromaffin Cell Membrane

Operationally we can distinguish only one type of voltage-dependent, noninactivating, inward Ca^{2+} current in cultured bovine adrenal chromaffin cells. The following results strongly support our claim that, under the experimental conditions described here, there is only one type of Ca^{2+} channel operat-

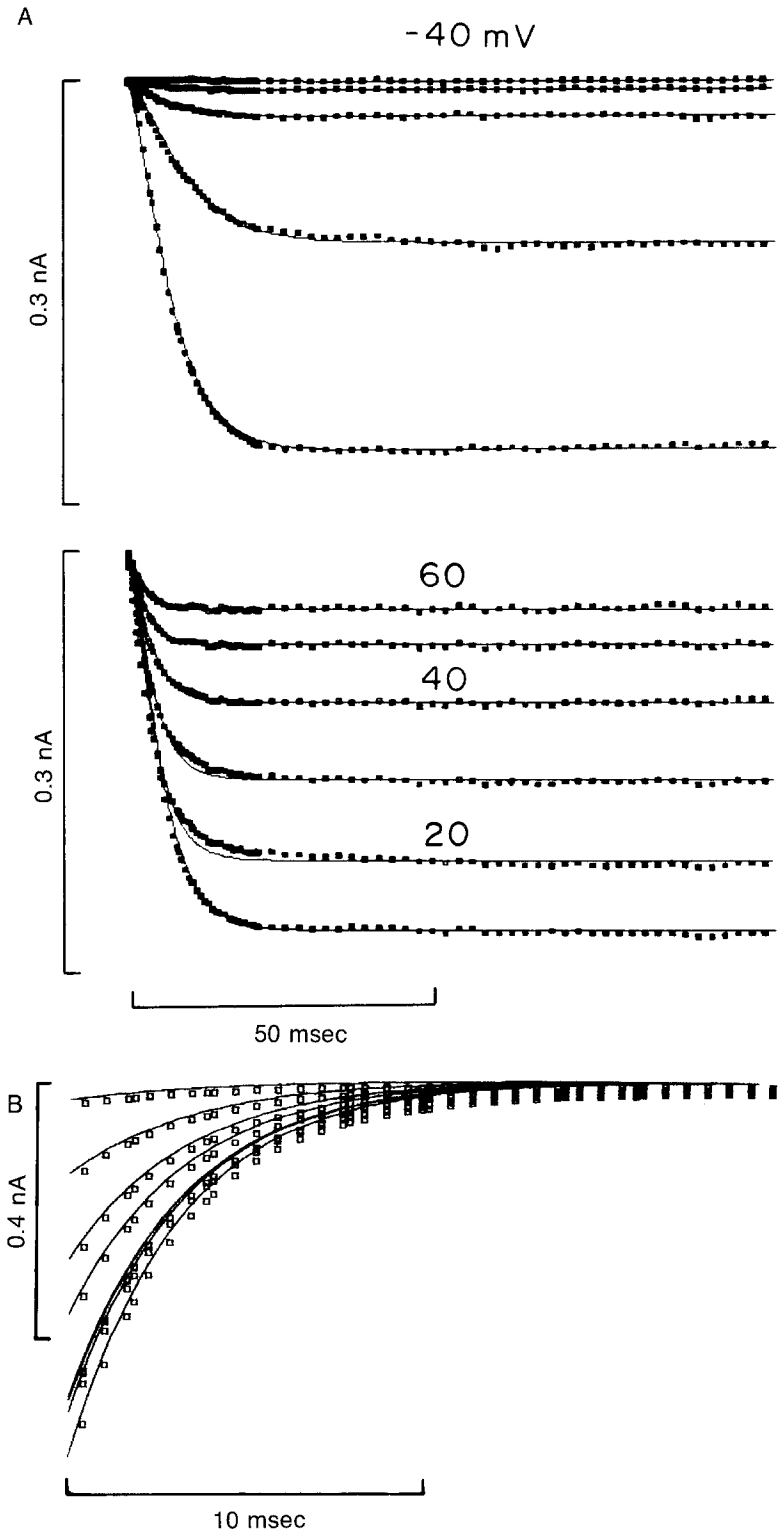

Fig. 8. Effect of BAY K-8644 on kinetic characteristics of the Ca^{2+} currents. (*A*) Symbols represent the experimental currents and solid curves represent model currents in BAY K-8644 (0.1 μM). For the initial part of each of the records, each symbol represents the average of three samples. (*B*) Tail currents on expanded time base. Solid lines were calculated as

$$i_{Ca}(t) = i_{Ca}(t = 0)\{\exp(-\beta(V = -80)t)\}^2.$$

The following values minimized the residual:

$V_{m,\text{pulse}}$ (mV)	$i_{Ca}(t = 0)$ (nA)	$\beta(V = -80)$ (sec^{-1})
−10	−0.02	115.0
0	−0.15	138.4
10	−0.28	146.9
20	−0.36	149.4
30	−0.49	152.3
40	−0.50	153.7
50	−0.51	154.2
60	−0.58	154.5

The mean value of 145.5 (±13.6) sec^{-1} gives a mean time constant of 6.9 (±0.7) msec

ing in the cell. Firstly, the time course of the inward current during the pulses could be described by square law kinetics (Fig. 2*A*,*B*). Secondly, the tails of inward current upon repolarization also exhibited one component with square law kinetics (Fig. 2*C*). Thirdly, increasing $[Ca^{2+}]_o$ from the physiological level of 2.5 to 5.2 mM did not significantly alter the kinetics of the currents during and after the pulses. However, the amplitude of the current increased as the concentration of the charge carrier was

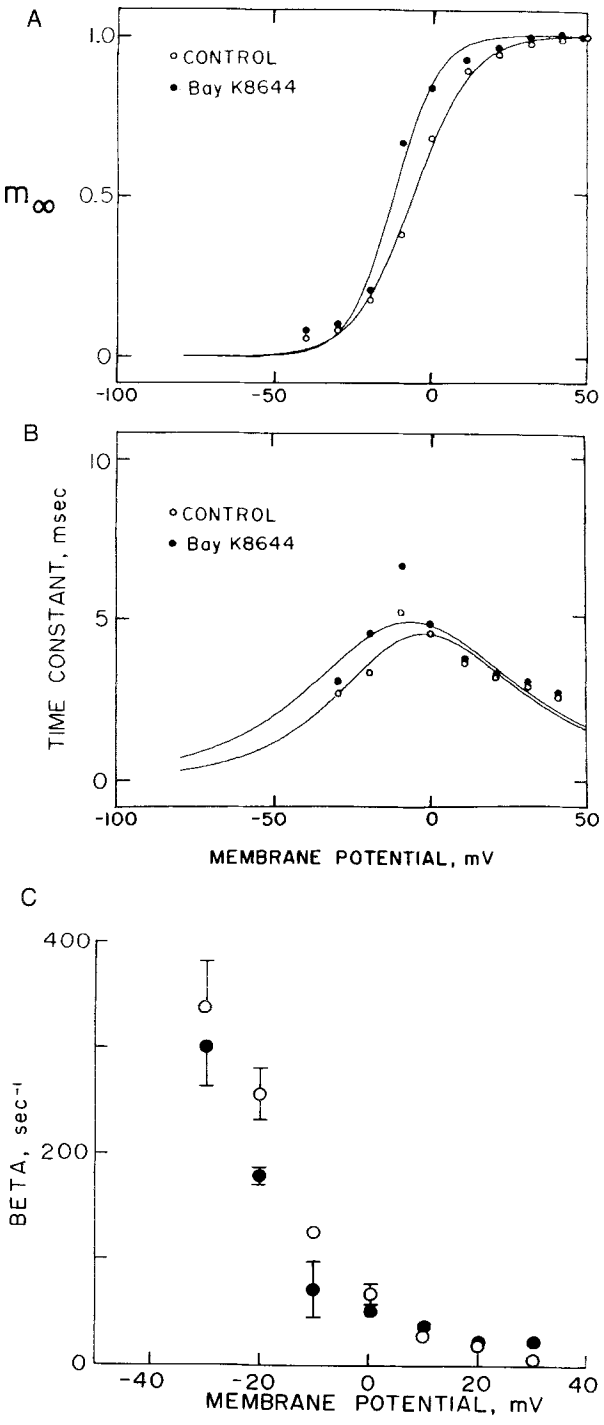

Fig. 9. Effects of BAY K-8644 (0.1 μM) on the steady-state open Ca^{2+}-channel probability and time constant curves. (*A*) m_∞ curves were calculated from the *I-V* curves using the equation given in the legend to Fig. 3. Parameters for the best fit in the presence of BAY K-8644 (●): $a = -3.6$, $V_o = -12.9$ mV. Control curve the same as for Fig. 3*A*. (*B*) Symbols represent mean values ($n = 4$) of the time constant for the activation calcium current. Fitted curve was calculated with the following parameters for the best fit: $A = 95$ sec^{-1}, $a = -0.72$, $V_o = -14.8$ mV, $B = 38$ msec^{-1}, $b = -0.99$ and $V_o = 13.5$. (*C*) Effect of BAY K-8644 on the rate constant for turning off the Ca^{2+} permeability. Values for the rate constants were calculated using Eqs. (4) and (5). Symbols represent the mean values ± SEM. Changes in $\alpha(V)$ values in Bay K-8644 were not significant as follows:

(n)	V (mV)	(V) (sec^{-1}) Control (2.5 mM Ca^{2+})	Bay K-8644 (0.1 μM)
1	−40	26.2 ± 5.1	19.5
3	−30	38.1 ± 9.5	29.4 ± 6.7
4	−20	43.4 ± 10.2	45.3 ± 2.6
4	−10	67.8 ± 10.9	78.5 ± 9.6
4	0	136.2 ± 16.2	165.7 ± 12.2
4	10	240.0 ± 20.6	232.6 ± 10.0
4	20	289.1 ± 22.2	284.5 ± 10.7
4	30	338.5 ± 35.3	301.1 ± 24.6
3	40	355.5 ± 49.0	380.7 ± 8.6

n: number of determinations from four different cells

increased following the independence principle (Hodgkin & Huxley, 1952*a*; Hodgkin & Katz, 1949). Activation of more than one Ca^{2+} channel is likely to generate currents with complex kinetics. Since the presence of different components in the current records would be readily detectable in our analysis and we have not been able to resolve more than one component with square law kinetics in all the records considered here, we conclude that only one type of Ca^{2+}-channel is active under our experimental conditions.

In nerve fibers high $[Ca^{2+}]_o$ causes a shift of the midpoint for the activation of the i_{Na} along the potential axis in the positive direction (Frankenhaeuser & Hodgkin, 1957). However, in the present series of experiments an elevation of $[Ca^{2+}]_o$ from 2.5 to 5.2 mM induced a significant shift of the midpoint of the activation curve for i_{Ca} in the opposite direction (Fig. 3*A*). To explain the Ca^{2+} induced shift Frankenhaeuser and Hodgkin (1957) made the assumption that Ca^{2+} neutralized fixed negative charges on the outer aspect of the axon membrane. In line with this interpretation, we can assume here the existence of such negative charges on the chromaffin cell membrane. We may further assume that augmenting $[Ca^{2+}]_o$ causes a reversal of the surface charge (Kruyt, 1952). In the model used for our analysis the midpoint potential for the activation curve V_o changes with the surface potential of the outer aspect of the membrane ψ_o as

$$V_o = \psi_i - \psi_o \tag{7}$$

where ψ_i is surface potential of the inner side of the membrane (Rojas, 1975). At physiological $[Ca^{2+}]_o$ (2.5 mM) V_o is close to −7 mV (Fig. 3*A*) and at 5.2 mM V_o is shifted to −11 mV (Fig. 3*B*). From Eq. (7), assuming that ψ_i remains unchanged, a reversal of the surface charge (or ψ_o) will cause a shift of the midpoint potential towards more negative values.

Identification of this Channel with the L Type

We have shown that either internal or external application of the Ca^{2+}-channel agonist Bay K-8644 induces a substantial increase in the size of the inward currents. At least four factors may contribute to this macroscopic effect of the dihydropyridine: (i) decrease in the rate constant for turning off the Ca^{2+} channel, (ii) increase in the rate constant for activation of the channel, (iii) increase in the amplitude of the single channel current and, (iv) increase in the number of channels available to conduct Ca^{2+} current. Our kinetic analysis of the macroscopic currents revealed that the rate constant for turning off the Ca^{2+} current, β, derived from the model, was significantly smaller at -10 and -20 mV in cells treated with the Ca^{2+}-channel agonist. Furthermore, our results demonstrate that $\alpha(V)$ is not affected by Bay K-8644 at 0.1 μM (*see* legend to Fig. 9). At the single Ca^{2+}-channel level these results indicate that the channel tended to remain in the open configuration. Our interpretation is in perfect agreement with direct observations of the effects of Bay K-8644 on the L-type Ca^{2+} channel in other cell types (Tsien et al., 1987; Kaczmarek, 1988). The Bay K-8644 dose-response curve in terms of chord conductance (Fig. 7) showed that, depending on concentration, this dihydropyridine acts on the chromaffin cell Ca^{2+} channel either as agonist (K_D = 0.027 μM) or as antagonist (K_D = 1.04 μM).

These properties, namely the presence of a single, noninactivating component in the currents and the sensitivity to the dihydropyridine Bay K-8644, taken together operationally define the Ca^{2+} channel present in the chromaffin cell membrane as L type (Tsien et al., 1987).

Bay K-8644 Increases the Voltage-Sensitivity of the Ca^{2+} Channel

The open probability curve for the Ca^{2+} channel in cells treated with Bay K-8644 is steeper than that from the control cells. Assuming a Boltzmann distribution of the channel between the open-closed configurations, we can calculate the necessary change in the size of the effective valence which would account for the observed effect (Fig. 9). The net increase was close to one electronic charge. A tentative explanation for this effect is that the Ca^{2+}-channel agonist stabilized the phosphorylated conformation of the channel (Chad, Kalman & Armstrong, 1987; Sperelakis & Wahler, 1988; Kaczmarek, 1988; O'Callahan & Hosey, 1988). Since, at least in principle, there should be a net gain of two electronic charges per phosphorylated site, using our protocols one might expect to detect the effect of added charges on the open probability cures.

Dual Action of Bay K-8644 on Calcium Channels

Studies on dihydropyridine inhibition of secretion have generated conflicting evidence regarding their efficacy in blocking both high K^+ and receptor-operated catecholamine secretion (Rosario et al., 1989). The dihydropyridine tested include nifedipine and nitrendipine (Malaisse & Boschero, 1977; Ceña et al., 1983; Malaisse-Lagae, Mathias & Malaisse, 1984). In contrast, Bay K-8644 systematically enhances both Ca^{2+} uptake and secretion in all studies published (Garcia et al., 1984; Malaisse-Lagae, Sener & Malaisse, 1986). In the present work we have attempted to resolve this issue by a systematic study on the kinetic consequences of Bay K-8644 action on Ca^{2+} currents. We found that, depending on concentration, Bay K-8644 can act as agonist (<0.1 μM) or atagonist (>1 μM). Our studies also showed that the enhancement of the inward current is the result of a reduction in the size of the rate constant to deactivate the Ca^{2+} current, the rate constant for activation remaining unmodified. Furthermore, we have shown that in the presence of Bay K-8644 (0.1 μM) the activation curve is steeper and shifted along the voltage axis towards more negative potentials. We also know that these two features of the Bay K-8644 action remain unmodified at higher concentrations, when the dihydropyridine is acting as a Ca^{2+}-channel antagonist (*data not shown*). This result supports our idea of the existence of two operationally different receptors for the dihydropyridines on the inner aspect of the Ca^{2+} channel.

We used Clark's occupancy theory (Boeynaems & Dumont, 1980) to obtain a function which we used to fit the dose-response data (Fig. 7). We assumed that: (i) there are two different receptors for Bay K-8644; (ii) the interaction between Bay K-8644 and each of these two receptors is reversible; (iii) all receptors are equivalent and independent; and (iv) the occupancy of a receptor does not modify the affinity for Bay K-8644 of the remaining free-receptors. It was further assumed that: (*v*) the change in chord conductance is proportional to the number of occupied receptors. The empirical function used to fit the points was calculated as

$$g_{Ca} = g_{Ca,max}\{1 + [B]/(K_{D,1} + [B])\}\{1 - [B]/(K_{D,2} + [B])\} + g^*_{Ca} \quad (8)$$

where [B] represents the concentration of Bay K-8644 and, g^*_{Ca} represents a component of the calcium conductance which is resistant to Bay K-8644, $K_{D,1}$ the dissociation constant for the receptor which is responsible for the agonist action and, $K_{D,2}$ the dissociation constant for the other receptor. The least-squares regression fit generated values for the

dissociation constants as 0.027 and 1 μM for the high and low affinity receptors, respectively. It should be noticed that the association of Bay K-8644 with the high affinity Ca^{2+}-channel activator site is defined by the term $\{1 + [B]/(K_{D,1} + [B])\}$. The association of Bay K-8644 with the inhibitory site is defined by the other term, namely $\{1 - [B]/(K_{D,2} + [B])\}$. Furthermore, interaction of the drug with the low affinity site leads to blockade of the channel.

Additional support for our interpretation of the dose-response curve was provided by our unpublished observations that, although nifedipine behaved as a poor antagonist (>5 μM) of the Ca^{2+} current, both the kinetics of the currents and the steady-state open probability curve for the Ca^{2+} channel remained unmodified.

References

Baker, P.F., Knight, D.E. 1984. Calcium control of exocytosis in bovine adrenal medullary cells. *Trends Neurosci.* **7:**120–125

Boeynaems, J.M., Dumont, J.E. 1980. Outlines of Receptor Theory. Elsevier/North-Holland Biomedical, Amsterdam

Ceña, V., Nicolas, P., Sanchez-Garcia, S.M., Kirpekar, S.M. Garcia, A.G. 1983. Pharmacological dissection of receptor-associated and voltage-sensitive ionic channels involved in catecholamine release. *Neuroscience* **10:**1455–1461

Chad, J., Kalman, D., Armstrong, D. 1987. The role of cyclic AMP-dependent phosphorylation in the maintenance and modulation of voltage-activated calcium channels. *Soc. Gen. Physiol. Ser.* **42:**167–186

Garcia, A.G., Sala, F., Reig, J.A., Viniegra, S., Frias, J., Fonteriz, R., Gandia, L. 1984. Dihydropyridine Bay K-8644 activates chromaffin cell calcium channels. *Nature (London)* **309:**69–73

Fenwick, E.M., Marty, A., Neher, E. 1982*a*. Sodium and calcium channels in bovine chromaffin cells. *J. Physiol. (London)* **331:**599–635

Fenwick, E.M., Marty, A., Neher, E. 1982*b*. A patch-clamp study of bovine chromaffin cells and of their sensitivity to acetylcholine. *J. Physiol. (London)* **331:**577–597

Forsberg, E., Rojas, E., Pollard, H.B. 1985. Receptor enhancement of nicotine-induced catecholamine secretion may be mediated by phosphoinositide metabolism in bovine adrenal chromaffin cells. *J. Biol. Chem.* **261:**4915–4922

Frankenhaeuser, B., Hodgkin, A.L. 1957. The action of calcium on the electrical properties of squid axons. *J. Physiol. (London)* **137:**218–244

Greenberg, A., Zinder, O. 1982. Catecholamine secretion from isolated adrenal medulla cells. *Cell Tissue Res.* **226:**655–665

Heldman, E., Levine, M., Morita, K., Pollard, H.B. 1989. Osmotic strength differentiates between two types of calcium transport pathways regulating CA secretion from cultured bovine chromaffin cells. *Biochim. Biophys. Acta (in press)*

Hodgkin, A.L., Huxley, A.F. 1952*a*. Currents carried by sodium and potassium ions through the membrane of the giant axon of *Loligo*. *J. Physiol. (London)* **116:**449–472

Hodgkin, A.L., Huxley, A.F. 1952*b*. A quantitative description of membrane current and its application to conduction and excitation in nerve. *J. Physiol. (London)* **117:**500–544

Hodgkin, A.L., Katz, B. 1949. The effect of sodium ions on the electrical activity of the giant axon of the squid. *J. Physiol. (London)* **108:**37–77

Holtz, R.W., Senter, R.A., Frve, R.A. 1982. Relationship between Ca^{2+} uptake and catecholamine secretion in primary dissociated cultures of adrenal medulla. *J. Neurochem.* **39:**635–646

Kaczmarek, L.K. 1988. The regulation of neuronal calcium and potassium channels by protein phosphorylation. *Adv. Sec. Messenger Phosphoprotein Res.* **22:**113–138

Kao, L.S., Schneider, A.S. 1985. Muscarinic receptors on bovine chromaffin cells mediate a rise in cytosolic calcium that is independent of extracellular calcium. *J. Biol. Chem.* **260:**2019–2022

Kidokoro, Y., Ritchie, A.K. 1980. Chromaffin cell action potentials and their possible role in adrenaline secretion from rat adrenal medulla. *J. Physiol. (London)* **307:**199–216

Kilpatrick, D.L., Ledbetter, F.H., Carson, K.A., Kirshner, A.G., Slepetis, R., Kirshner, N. 1980. Stability of bovine adrenal medulla cells in culture. *J. Neurochem.* **35(3):**679–692

Kruyt, H.R. 1952. Colloid Science. Vol. 1. Elsevier, Amsterdam

Malaisse, W.J., Boschero, A.C. 1977. Calcium antagonists and islet function: XI. Effects of nifedipine. Horm. Res. **8:**203–209

Malaisse-Lagae, F., Mathias, P.C.F., Malaisse, W.J. 1984. Gating and blocking of calcium channels by dihydropyridines in the pancreatic B-cell. *Biochem. Biophys. Res. Commun.* **123:**1062–1068

O'Callahan, C.M., Hosey, M.M. 1988. Multiple phosporylation sites in the 165-kilodalton peptide associated with dihydropyridine-sensitive calcium-channels. *Biochemistry* **27:**6071–6077

Pollard, H.B., Brocklehurst, K.W., Forsberg, E., Stutzin, A., Lee, G., Burns, A.L. 1986. Calcium regulation of membrane fusion during hormone secretion *Adv. Exp. Med. Biol.* **211:**369–384

Quinta-Ferreira, M.E., Rojas, E., Arispe, N. 1982. Potassium currents in the giant axon of the crab *Carcinus maenas*. *J. Membrane Biol.* **66:**171–181

Rojas, E. 1975. Gating mechanism for the activation of the sodium conductance in nerve membranes. *Cold Spring Harbor Symp. Quant. Biol.* **40:**305–320

Rosario, L.M., Soria, B., Feuerstein, G., Pollard, H.B. 1989. Evidence that chromaffin cells have voltage-sensitive calcium channels insensitive to dihydropyridines or omega-conotoxin. *Neuroscience (in press)*

Sakmann, B., Neher, E. 1983. Single-channel Recording. Plenum, New York

Schneider, A.S., Cline, H.T., Rosenbeck, K., Sonenberg, M. 1981. Stimulus-secretion coupling in isolated chromaffin cells: Calcium-channel activation and possible role of cytoskeletal elements. *J. Neurochem.* **37(3):**567–575

Sperelakis, N., Wahler, G.M. 1988. Regulation of Ca^{2+} influx in myocardial cells by beta adrenergic receptors, cyclic nucleotides, and phosphorylation. *Mol. Cell. Biochem.* **82:**19–28

Stutzin, A., Stojilkovic, S., Catt, K.J., Rojas, E. 1989. Characteristics of two types of calcium channels in the plasma membrane of rat pituitary gonadotrophs. *Am. J. Physiol. (in press)*

Tsien, R.W., Hess, P., McCleskey, E.W., Rosenberg, R.L. 1987. Calcium channels: Mechanisms of selectivity, permeation, and block. *Annu. Rev. Biophys. Chem.* **16:**265–290

Received 25 May 1989; revised 25 August 1989